Optimal Deflection of Resonant Near-Earth Objects Using the B-Plane

Mathieu Petit and Camilla Colombo

Abstract A very large number of asteroids populates our Solar System; some of these are classified as Near Earth Objects (NEO), celestial bodies whose orbit lies close to or even intersects our planet's, a few of which are believed to pose a potential threat for Earth. Their hazardous nature has caught the eye of both the public and the scientific community and the concern has grown over the past decades, followed by a multitude of studies on the different aspects that characterise this problem. The most common solution that has been proposed in order to face a potential impact situation is the deflection of incoming asteroids in such a way that their encounter with the Earth is avoided or modified to an extent that it does not pose a threat through a kinetic impactor. The present article will expand on previous works in this sector, with the aim of defining an optimal orbit deviation strategy with the objective of not only avoiding the incumbent close-encounter, but to also reduce the risk of a future return of the NEO to the Earth. To this purpose, the effect of the deflection will be studied by means of the b-plane, a very convenient reference frame used to characterise an encounter between two celestial bodies, to determine a deflection strategy that will avoid the conditions corresponding to a resonant return of the asteroid to the Earth. The results presented in this work feature an analytical correlation between the deflection action and the resulting displacement along the axes of the b-plane and the description of optimal deflection techniques based on the aforementioned formulas. Finally, a numerical implementation of the deflection strategy demonstrates its effectiveness when applied to a test scenario.

Mathieu Petit
MSc Graduate in Space Engineering, Department of Aerospace Science and Technology, Politecnico di Milano, Via La Masa, 34 20156 Milano, mathieu.petit@mail.polimi.it

Camilla Colombo, PhD
Associate Professor, Department of Aerospace Science and Technology, Politecnico di Milano, Via La Masa, 34 20156 Milano, camilla.colombo@polimi.it

1 Introduction

Asteroids and comets are celestial bodies mainly composed by rocks and ice respectively. While they are very interesting from a scientific point of view, as their properties are largely unchanged since the time of the planets' formation, they can present a very significant danger for life on Earth in the case of an impact on the surface of our planet. The objects that could pose such a threat belong to the Near-Earth Object (NEO) family, defined as asteroids and comets with a perihelion distance of less than 1.2 AU [1]. Most NEOs are asteroids, referred to therefore as Near-Earth Asteroids (NEAs). The most dangerous NEAs also belong to the class of Potentially Hazardous Asteroids (PHAs), which feature a Minimum Orbit Intersection Distance (MOID), the minimum geometric distance between two orbits, of less than 0.05 AU and an absolute magnitude of 22.0 or brighter [1]. Of the over than 600,000 known asteroids, more than 16,000 are classified as NEOs, of which in turn around 10% fall in the category of PHAs [2]. Despite the seemingly high numbers, the probability of an impact is low, but the damage it could produce is very significant [3].

Another aspect of this threat is represented by the possibility of a NEO which has already flown close to the Earth to return to our planet a few years down the line. This phenomenon is known as a resonant return [4] and is determined by the possibility of a first close approach to deviate a small body's orbit in such a way that the new orbit will lead to a future encounter. A notable case of this effect is represented by asteroid 2010 RF_{12}, a PHA discovered during a close approach in 2010, which will return to our planet several times in the future. The closest of these encounters is predicted around the 6th of September 2095, where it will approach the Earth as close as $1.209 \cdot 10^{-4}$ AU [5].

In this article, the kinetic impactor strategy will be considered as the sole deflection technique in awe of its relative simplicity and ease of correlation with the obtained deflection. This is in line with the UN-mandated Space Mission Planning Advisory Group's (SMPAG) statement defining the kinetic impactor as the most viable deflection technique at this stage [6]. Furthermore, its modelling will be carried out in a simplified manner, neglecting effects due to momentum dissipation and non-uniform composition of the target, as well as the effect of a possibly uneven geometry paired with a rotation of the body [7]. The article is organised as follows: Sect. 2 describes the b-plane and its properties, Sect. 3 details the modelling used for the deflection and its effect on the encounter, as well as the optimal deflection strategy, Sect. 4 features a test case in which the aforementioned strategy is applied to the deflection of a NEO and Sect. 5 contains the conclusions discussing the obtained results.

2 The B-Plane Representation

The b-plane, introduced by Öpik [8] and later studied by several authors [4] [7] [9], is a very convenient instrument used to characterise fly-bys; the qualities that determine its advantages will be illustrated in Sect. 2.1, followed by some considerations on the tools specific to this reference frame, upon which this work is based. Finally, a section containing the obtained results inherent to resonant returns, as determined through the b-plane itself, will conclude this section.

2.1 B-Plane Definition

The b-plane is a planetocentric reference frame $\{\xi,\eta,\zeta\}$, such that ξ and ζ are coordinates on the b-plane and η is normal to this plane. The direction of the η-axis is identified by the planetocentric velocity vector $\boldsymbol{u}$, whereas the ζ-axis is directed in the opposite direction as the projection of the planet's velocity vector on the b-plane and the ξ-axis completes the right-handed reference frame [8]. The impact parameter is the intersection of the incoming hyperbola asymptote with the b-plane and is therefore defined as

$$b = \sqrt{\xi^2 + \zeta^2}$$

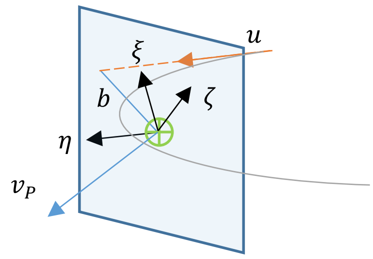

Fig. 2.1 B-plane geometry

The b-plane has the very useful property to conveniently characterise close approaches between an object and a planet, as it decouples the two main parameters that describe the encounter: the geometric distance and the timing of the close-approach. It can be shown that the ξ-axis represents the geometric distance between the two bodies' orbits at the encounter, whereas the ζ-axis represents a shift in the time of arrival of the object at the planet [4]; a positive value of ζ represents a delay and vice-versa for a negative value of the coordinate. The aforementioned properties are based on the approximation that, at the time of the encounter, the two orbits are straight lines [9].

Two different b-planes can be drawn for an encounter when considering a patched-conics approach: the one referred to the incoming asymptote of the hyperbola and the one relative to the outgoing one.

2.2 Öpik's Theory

Öpik's theory for planetary encounters is based on a patched two-body approach. The object is considered to be on its heliocentric orbit until it encounters the planet, where it transitions to a hyperbolic orbit under the sole attraction of the planet and finally returns to a different heliocentric orbit. As the effect of the encounter is considered as an instantaneous deflection of the object's velocity vector from its incoming asymptote to its outgoing one, Öpik's theory is more accurate for deep encounters. This is due to the planetocentric velocity of the object being higher, thus better approximated by a point-like interaction [10].

2.2.1 Planetocentric Reference Frame

The following planetocentric reference frame (see Fig. 2.2) is central to the discussion of Öpik's theory; it is based on the hypothesis of the planet being on a circular orbit around the Sun and is defined as follows: *X*-axis directed along the position vector of the planet with respect to the Sun, *Y*-axis in the direction of the planet's velocity vector and *Z*-axis completing the right-handed frame.

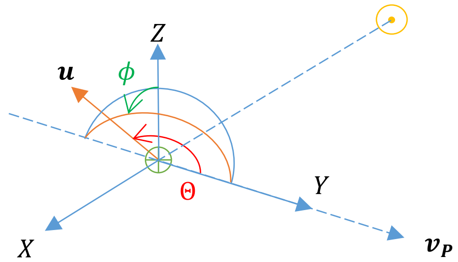

Fig. 2.2 Planetocentric reference frame

Vectors in the planetocentric reference frame are described by means of the angles Θ and ϕ, following the notation used by Valsecchi et al. [4], represented in Fig. 2.2. Öpik's theory cannot be used in the case of exactly tangent and coplanar orbits and the results become unreliable for orbits approaching these conditions, corresponding to $\sin\Theta \simeq 0$ [4] [10].

2.2.2 B-Plane Tools

While an extension of Öpik's original theory was formulated by Valsecchi et al. [4] allowing for its use in the case of near misses; a numerical approach has been implemented in the present work, to allow for the relaxing of some of the hypotheses (see Sect. 2.4). Nevertheless, many of the results obtained by Valsecchi et al.

[4] will be used to characterise the encounter and the theoretical return conditions predicted by Öpik's theory [8]. Amongst these are the description of the planetocentric velocity of the object in the planetocentric reference frame and the computations required to obtain the post-flyby velocity vector and position on the b-plane [11].

2.3 Resonant Returns

2.3.1 Resonant Return Circles

To witness a planetary encounter of the object, under the assumption of Keplerian motion between the two close-approaches, the following condition must be satisfied

$$kT_P = hT'$$

where T_P and T' are the periods of the planet and the object after the encounter respectively and k and h are integer numbers. Following this approach and considering the tools discussed in Sect. 2.2.2, a circle can be drawn on the b-plane for each couple of values h and k corresponding to a return condition of the small body to the planet [4]. These circles are referred to as resonance circles, as they represent the loci of orbits that will bring the object back to the planet after a certain amount of revolutions of both bodies.

A convenient notation for the resonant circles is (h,k), to represent the number of periods of the deflected small body and the planet necessary to obtain the return respectively. This notation can also be applied to the corresponding keyholes, described in Sect. 2.3.2.

The formulation described in this work is based on the assumption that the small body's position coincides with that of the planet with respect to the Sun, as per Öpik's classical theory [8]. However, this simplification still provides a good approximation of the resonance conditions, as the higher-order terms in ξ and ζ, which are present when relaxing the aforementioned hypothesis, is limited to a slight distortion of the circles [4]. Nevertheless, the conditions corresponding to a return of an object to the planet portrayed in the results of this work will be computed numerically in order to guarantee the expected returns (see Sect. 2.4).

Circles with a value of the radius $R < \xi_b$ are considered as dynamically unreachable, as ξ_b is the value of ξ of the incoming trajectory and it is the minimum value that the impact parameter can reach in the case that the two orbits are perfectly phased (i.e. it corresponds to the MOID) [12].

Furthermore, resonant circles can theoretically be drawn for any couple of values (h,k). However, as the b-plane is built on the hypothesis of a two-body propagation, the circles corresponding to returns that would be very distant in time cannot be considered as representative of the real conditions. A value of $h = k = 10$ is a reasonable limit for the choice of resonant circles [9] [13].

2.3.2 Keyholes

The keyholes are the regions of the b-plane that will bring to a subsequent encounter, were the asteroid to pass through one of them. They can represent either a hit, in which case they are none-other than the pre-images of the planet's cross-section at the second encounter on the b-plane of the first, or more generally a subsequent close-encounter (for example the pre-image of the SOI's cross-section) [4].

Per their nature, keyholes are linked to the semi-major axis of the asteroid after the first fly-by and thus are located in the vicinity of the resonant circles corresponding to their anticipated return. In the case of a purely Keplerian propagation between the encounters, the only b-plane coordinate to vary is ζ, as it is related to the timing of the encounter, whereas the geometry of the orbit (i.e. the MOID) is unaffected [4].

The size of keyholes varies based on two main parameters: the distance from the ξ-axis and the number of periods connected with the relative resonant circle [9]. Keyholes that are situated further from the ξ-axis are larger, as the effect of the fly-by varies more significantly in space when closer to the planet, leading to very different orbits. Keyholes connected to returns more distant in time are smaller, as the time difference at the encounter, due to a given difference in the period after the flyby, grows in time.

2.4 Numerical Keyhole Definition

This section will show the effect of the passage of a NEO through a keyhole during a fly-by of the Earth. As some hypotheses made in defining the resonance circles and the relative keyholes in the framework of Öpik's theory [8] have been relaxed, namely the circularity of the Earth's orbit and the coincidence of the NEO and the planet with respect to the Sun during the encounter [4], the precise keyholes have been computed numerically through the following algorithm developed in this work and inspired on Bourdoux's work [9]:

1. The nominal encounter between the asteroid and the planet is recorded (a two-body propagation is assumed for both the Earth and the NEO), based on the entrance of the asteroid in the planet's SOI
2. An array of values of ζ is explored to analyse the period of the corresponding orbit after the fly-by, while keeping the value of the ξ coordinate constant and equal to its nominal value (corresponding to a shift in time of the encounter)

3. If the resulting post-encounter semi-major axis corresponds to a value of the period required for a resonant return after h periods of the NEO and k periods of the Earth, given a certain tolerance, the value of ζ is recorded as being part of the (h,k) keyhole

The reason for which the position and size of the keyhole is computed along the ζ direction stems from the knowledge that we have of the NEOs' orbital parameters. In practice, small differences in the semi-major axis of an asteroid can have a very significant effect on the timing of an encounter when the coordinates are propagated for a long integration time [9]. Furthermore, as will be illustrated in Sect. 3, in most cases, the deflection along the ζ-axis dominates over the one along the ξ-axis.

Fig. 2.3 depicts both the analytical resonant circles (grey circles) and the numerically computed keyholes (orange arcs); the keyholes have been computed considering a variation of the nominal encounter conditions along the ξ-axis, in addition to the one along the ζ-axis, to better illustrate the effect. It can be seen that, while the shape of the numerical keyholes closely resembles that of the analytical resonant circles, their positions on the b-plane are significantly different in awe of the different hypotheses on which they are based.

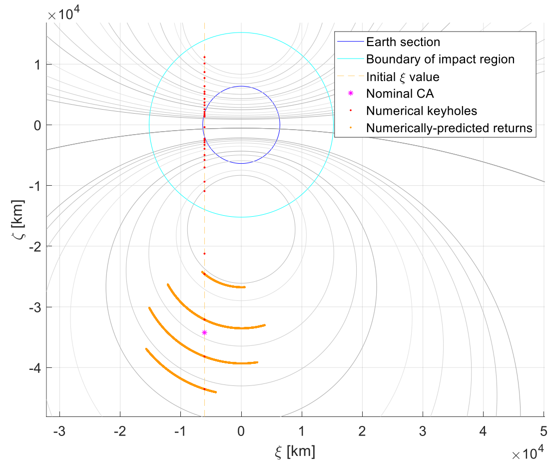

Fig. 2.3 B-plane representation of the 2095 encounter between 2010 RF_{12} and the Earth; the keyholes have been obtained numerically through the described technique

2.5 Effect of the Keyholes

The following example analyses the encounter between asteroid 2010 RF_{12} and the Earth expected on the 6th of September 2095 [5]. The choice of the NEO is based on 2010 RF_{12} currently having the highest probability of colliding with the Earth amongst the known PHAs, estimated at around 6% for the selected encounter [5].

Table 1 shows the Keplerian parameters assumed for this example (where MJD2000 is the modified Julian date), obtained through NASA SPICE [14] and propagated considering a two-body problem framework.

Table 1 Keplerian parameters of the Earth and the asteroid assumed for this example

	a [km]	e	i [rad]	Ω [rad]	ω [rad]	θ [rad]	MJD2000
Earth	$1.4972 \cdot 10^8$	0.0164	$2.0800 \cdot 10^{-4}$	3.05	4.99	4.13	$3.4942 \cdot 10^4$
2010 RF_{12}	$1.5739 \cdot 10^8$	0.1881	0.0160	2.8	4.66	4.68	$3.4942 \cdot 10^4$

Three new initial synthetic conditions corresponding to different values of ζ on the pre-encounter b-plane are obtained by keeping the other quantities defining the b-plane unchanged (U, Θ, θ and ξ) with respect to the nominal encounter: the centre of keyhole (5,4), the centre of keyhole (6,5) and the middle point between these two keyholes. The numerical propagation of the synthetic initial conditions is displayed in Fig. 2.4. As expected from the initial conditions, the encounters crossing the keyholes (red and green lines) feature Earth returns after the corresponding numbers of periods of the asteroid and the Earth, whereas the point halfway between the considered keyholes (blue line) does not feature an Earth return in the considered timeframe (based on the maximum resonant return considered when calculating the position and size of the keyholes). This condition is therefore *desirable* for the deviation of an incoming asteroid, as will be discussed in Sect. 4.1.

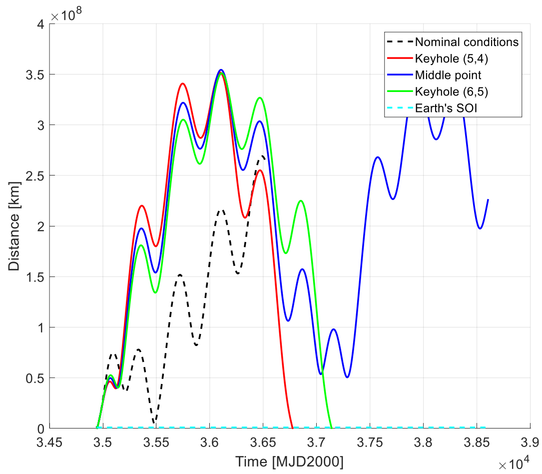

Fig. 2.4 Distance between 2010 RF_{12} and the Earth for the considered initial conditions (the keyholes lead to the expected returns)

2.5.1 Validity of the Approach

We need to consider that the analysis performed so far is conducted in the patched-conics method of the Restricted Two-Body Problem (R2BP). In reality, NEOs' orbits need to be propagated in the n-Body Problem (nBP) considering the presence of the Solar System planets [11]. Nevertheless, the proposed simplified approach can be considered as a viable first approximation for the real case, as the results of the R2BP approximation are indicative of the real situation on the short period (up to 10 years approximatively, as stated in Sect. 2.3.1).

3 Near-Earth Object Deflection

This section will describe the modelling approach for the deflection manoeuvre and the resulting displacement at the MOID. The maximisation of the deflection effect will be discussed considering different objectives, both purely geometrical and concerning the b-plane properties. Finally some results relative to the proposed techniques will be presented to corroborate the theoretical results.

3.1 Deflection Model

The objective of the deviation action is to cause a displacement of the NEO at the time of the close approach through an impulsive manoeuvre at a time t_d. The first step in defining the required optimisation strategy is to detail the equations applied to the modelling of the deflection. The approach used in this part of the work was proposed by Vasile and Colombo [7] and is here expanded to consider the projection of the deflection on the b-plane.

As the perturbed orbit can be considered proximal to the original one, the position of the NEO after the deviation can be computed through the use of the proximal motion equations in function of the variation of the orbital parameters due to the deflection [7], which in turn can be determined through the Gauss planetary equations derived for finite differences, if an instantaneous perturbation of the NEO velocity vector is considered. This method provides a relatively simple and computationally inexpensive strategy to determine the effect of a deviation [7].

Given the vector scheme in Fig. 3.1, Δr represents the nominal distance between the NEO and the planet at the MOID, while δr is the displacement from the nominal conditions due to the deflection.

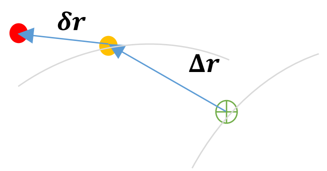

Fig. 3.1 Distance vectors at the MOID (Earth in green, non-deviated NEO in orange and deviated NEO in red)

By combining the proximal motion equations and the Gauss planetary ones, the following matrix formulation linking the deflection impulse velocity vector $\boldsymbol{\delta v}$ at the deflection point to the deviation vector $\boldsymbol{\delta r}$ at the MOID can be obtained [7]:

$$\begin{cases} \boldsymbol{dr}_{MOID} = \boldsymbol{A}_{MOID}\boldsymbol{d\alpha}_d \\ \boldsymbol{\delta\alpha}_d = \boldsymbol{G}_d\boldsymbol{\delta v}_d \end{cases} \Rightarrow \boldsymbol{dr}_{MOID} = \boldsymbol{A}_{MOID}\boldsymbol{G}_d\boldsymbol{dv}_d = \boldsymbol{T}\boldsymbol{dv}_d \tag{3.1}$$

where $\boldsymbol{\delta\alpha}_d$ is the vector representing the variation of the orbital parameters due to the deflection action.

It should be noted that the equations presented in this formulation are consistent with a Keplerian motion of the involved bodies along elliptical and quasi-circular orbits [15]. Even though the deviation is evaluated at the MOID, the formulas presented in this section (and applied in the following sections) remain valid in the case the encounter is not correctly phased and therefore does not take place at the exact MOID; this is due to the fact that the encounter is assumed to take place at the MOID in the present formulation, but no related restriction is applied to the formulas (i.e. the MOID represents the close-encounter conditions).

3.2 Maximisation of the Deflection

3.2.1 Geometric Deviation

As proposed and applied by Colombo [15] to NEO deflection missions, a convenient formulation to maximise the relative deviation $\|\boldsymbol{\delta r}_{MOID}\|$ is based on maximising the quadratic form $\boldsymbol{T}^T\boldsymbol{T}$ associated with (3.1). This can be achieved by choosing an impulse velocity vector $\boldsymbol{\delta v}_d$ parallel to the direction of the eigenvector of the matrix $\boldsymbol{T}^T\boldsymbol{T}$ conjugated to its maximum eigenvalue. This method only constrains the direction of $\boldsymbol{\delta v}_d$ while its sign can be chosen to determine the direction of the corresponding displacement [7]. The sign is therefore selected such that the deviation increases the distance of the asteroid from the Earth at the time of the encounter.

3.2.2 Deviation on the B-Plane

The method applied to the maximisation of the geometric deviation is extended in this paper to maximise both the deviation of the impact parameter $\boldsymbol{\delta b}_{MOID}$ and the single components on the b-plane $\boldsymbol{\delta\xi}_{MOID}$ and $\boldsymbol{\delta\zeta}_{MOID}$. In order to use the previously described procedure, the quantities must be taken as vectors in space and expressed as the product of a matrix and the impulse velocity vector.

Let us consider the achieved deviation for the impact parameter *b* on the b-plane. To do so, the first step must be the computation of the deflection vector in the b-plane:

$$\boldsymbol{\delta b_{MOID}} = \boldsymbol{\delta r_{MOID}} - \left(\boldsymbol{\delta r_{MOID}} \times \boldsymbol{e_\eta}\right)\boldsymbol{e_\eta} \tag{3.2}$$

where $\boldsymbol{e_\eta}$ is the unitary vector of the η-axis of the b-plane and $\boldsymbol{\delta b_{MOID}}$ is a vector identifying δb_{MOID}, the deviation on the b-plane.

Considering the vector triple product identity, we have

$$\boldsymbol{e_\eta} \times \left(\boldsymbol{\delta r}_{MOID} \times \boldsymbol{e_\eta}\right) = \left(\boldsymbol{e_\eta} \cdot \boldsymbol{e_\eta}\right)\boldsymbol{\delta r}_{MOID} - \left(\boldsymbol{\delta r}_{MOID} \cdot \boldsymbol{e_\eta}\right)\boldsymbol{e_\eta} = \boldsymbol{\delta r}_{MOID} - \left(\boldsymbol{\delta r}_{MOID} \cdot \boldsymbol{e_\eta}\right)\boldsymbol{e_\eta}$$

We can therefore re-write (3.2) as

$$\boldsymbol{\delta b}_{MOID} = \boldsymbol{\delta r}_{MOID} - \boldsymbol{\delta r}_{MOID} + \boldsymbol{e_\eta} \times \left(\boldsymbol{\delta r}_{MOID} \times \boldsymbol{e_\eta}\right) = \boldsymbol{e_\eta} \times \left(\boldsymbol{\delta r}_{MOID} \times \boldsymbol{e_\eta}\right) \tag{3.3}$$

The previous expression can also be written in the compact form

$$\boldsymbol{\delta b}_{MOID} = \boldsymbol{M_{\delta b}} \boldsymbol{\delta r}_{MOID}$$

$$\boldsymbol{M_{\delta b}} = \begin{bmatrix} {e_{\eta 2}}^2 + {e_{\eta 3}}^2 & -e_{\eta 1}e_{\eta 2} & -e_{\eta 1}e_{\eta 3} \\ -e_{\eta 1}e_{\eta 2} & {e_{\eta 1}}^2 + {e_{\eta 3}}^2 & -e_{\eta 2}e_{\eta 3} \\ -e_{\eta 1}e_{\eta 3} & -e_{\eta 2}e_{\eta 3} & {e_{\eta 1}}^2 + {e_{\eta 2}}^2 \end{bmatrix}$$

where $e_{\eta i}$ are the components of the unitary vector $\boldsymbol{e_\eta}$.

The deviation on the b-plane $\boldsymbol{\delta b_{MOID}}$ can now be mapped to the deviation manoeuvre $\boldsymbol{\delta v_d}$:

$$\boldsymbol{\delta b}_{MOID} = \boldsymbol{M_{\delta b} T \delta v}_d = \boldsymbol{T_{\delta b} \delta v}_d \tag{3.4}$$

We have obtained an analytical formulation to describe the deviation on the b-plane at the MOID as a function of the deflection action, which can be used to obtain the direction of the maximum deviation on the b-plane through the optimisation technique of Sect. 3.2.1. This is the first innovative result continuing Vasile and Colombo's work [7], which relied on a numerical computation of δb_{MOID}.

Let us now compute the components of $\boldsymbol{\delta b_{MOID}}$ (from (3.4)) on the b-plane:

$$\boldsymbol{\delta\xi}_{MOID} = \boldsymbol{\delta b}_{MOID} - \left(\boldsymbol{\delta b}_{MOID} \cdot \boldsymbol{e}_\zeta\right)\boldsymbol{e}_\zeta,\ \boldsymbol{\delta\zeta}_{MOID} = \boldsymbol{\delta b}_{MOID} - \left(\boldsymbol{\delta b}_{MOID} \cdot \boldsymbol{e}_\xi\right)\boldsymbol{e}_\xi$$

where $\boldsymbol{e_\xi}$ and $\boldsymbol{e_\zeta}$ are the unitary vectors of the ξ and ζ axes of the b-plane respectively.

Through the same procedure applied for the impact parameter in (3.4), we can write

$$\boldsymbol{\delta\xi}_{MOID} = \boldsymbol{M_{\delta\xi}\delta b}_{MOID},\ \boldsymbol{\delta\zeta}_{MOID} = \boldsymbol{M_{\delta\zeta}\delta b}_{MOID}$$

$\boldsymbol{\delta\zeta_{MOID}}$ and $\boldsymbol{\delta\zeta_{MOID}}$ are the vectors representing the deflection along the respective axes on the b-plane.

$$\boldsymbol{M}_{\delta\xi} = \begin{bmatrix} e_{\zeta 2}{}^2 + e_{\zeta 3}{}^2 & -e_{\zeta 1}e_{\zeta 2} & -e_{\zeta 1}e_{\zeta 3} \\ -e_{\zeta 1}e_{\zeta 2} & e_{\zeta 1}{}^2 + e_{\zeta 3}{}^2 & -e_{\zeta 2}e_{\zeta 3} \\ -e_{\zeta 1}e_{\zeta 3} & -e_{\zeta 2}e_{\zeta 3} & e_{\zeta 1}{}^2 + e_{\zeta 2}{}^2 \end{bmatrix}, \boldsymbol{M}_{\delta\zeta} = \begin{bmatrix} e_{\xi 2}{}^2 + e_{\xi 3}{}^2 & -e_{\xi 1}e_{\xi 2} & -e_{\xi 1}e_{\xi 3} \\ -e_{\xi 1}e_{\xi 2} & e_{\xi 1}{}^2 + e_{\xi 3}{}^2 & -e_{\xi 2}e_{\xi 3} \\ -e_{\xi 1}e_{\xi 3} & -e_{\xi 2}e_{\xi 3} & e_{\xi 1}{}^2 + e_{\xi 2}{}^2 \end{bmatrix}$$

where $e_{\xi i}$ and $e_{\zeta i}$ are the components of the respective unit vectors.

The components of $\boldsymbol{\delta b_{MOID}}$ in the b-plane can therefore be written in a compact fm as:

$$\begin{aligned} \boldsymbol{\delta\xi}_{MOID} &= \boldsymbol{M}_{\delta\xi}\boldsymbol{T}_{\delta b}\boldsymbol{\delta v}_d = \boldsymbol{M}_{\delta\xi}\boldsymbol{M}_{\delta b}\boldsymbol{T}\boldsymbol{\delta v}_d = \boldsymbol{T}_{\delta\xi}\boldsymbol{\delta v}_d \\ \boldsymbol{\delta\zeta}_{MOID} &= \boldsymbol{M}_{\delta\zeta}\boldsymbol{T}_{\delta b}\boldsymbol{\delta v}_d = \boldsymbol{M}_{\delta\zeta}\boldsymbol{M}_{\delta b}\boldsymbol{T}\boldsymbol{\delta v}_d = \boldsymbol{T}_{\delta\zeta}\boldsymbol{\delta v}_d \end{aligned} \tag{3.5}$$

3.2.3 Maximisation of the Components in the B-Plane

The same method used in [15] to maximise the relative deviation $\|\boldsymbol{\delta r}_{MOID}\|$ based on maximising the quadratic form $\boldsymbol{T}^T\boldsymbol{T}$ associated with (3.1) can now be extended to maximise $\|\boldsymbol{\delta b}_{MOID}\|$, $\|\boldsymbol{\delta\xi}_{MOID}\|$ or $\|\boldsymbol{\delta\zeta}_{MOID}\|$. This can be achieved by choosing an impulse velocity vector $\boldsymbol{\delta v_d}$ parallel to the direction of the eigenvector of the matrix $\boldsymbol{T}_{sel}{}^T\boldsymbol{T}_{sel}$ (where $\boldsymbol{T}_{sel}$ is the matrix mapping the desired vector on the b-plane to the deflection action $\boldsymbol{\delta v_d}$, as described in Sect. 3.2.2) conjugated to its maximum eigenvalue. This method only constrains the direction of $\boldsymbol{\delta v_d}$ while its sign can be chosen to determine the direction of the corresponding displacement [7]. The sign is therefore selected such that the deviation increases the value of the selected coordinate (b, ξ or ζ) of the projection of the deflected encounter conditions on the b-plane.

Indeed, this method is used to compute the optimal direction of the deflection to be imparted to the asteroid as a function of the time before the possible impact Δt. Once the deflection direction has been defined, the magnitude of the velocity vector $\boldsymbol{\delta v_d}$ can be increased as much as possible to further deviate the NEO, but the optimal direction of deviation does not change.

3.2.4 Validation of the Eigenvector Method Extension

The aforementioned analytic maximisation technique of the different b-plane components has been successfully validated by comparing its results with the outcomes of a classical numerical optimisation, performed with MATLAB®'s *fmincon* optimiser (an optimiser based on the "interior point" algorithm). Furthermore, it has been shown that employing the analytical technique yields a considerable advantage from a computational time standpoint [11].

3.3 Optimal Deflection Direction

Asteroid 2010 RF_{12} was chosen as the test subject for this section. The ephemerides data for the PHA has been obtained from NASA SPICE [14]. Furthermore, the representation of the b-plane components is shown on the b-plane computed considering the unperturbed encounter of the NEO with the Earth, instead of the one relative to the perturbed relative velocity of the asteroid with respect to the Earth. This approach does not impair the outcome of the study as the plane perpendicular to the nominal relative velocity and the one perpendicular to the perturbed relative velocity are very close to each other [7].

3.3.1 Maximum Geometric and Impact Parameter Deviation

Fig. 3.2 shows the components of the optimal deviation direction for the NEO in function of the deflection time Δt, expressed as multiples of the asteroid's orbital period. The values of the components are expressed on a total norm of 1 (i.e. a normalised deflection vector is considered); this approach is equivalent to considering the dimensional velocity vector, as stated in Sect. 3.2.3.

Concerning the geometric deflection, the normal component is the preferred one for low values of Δt until a deviation time depending on the asteroid. From this point earlier (i.e. for longer deviation times), the tangent component is the most effective one [7]. It should be noted that a deviation in the normal direction would yield practically no result if performed at $\Delta t = kT_{NEO}$. The out-of-plane component's value is not shown, as it is below 10^{-13}.

The direction of maximum δb increase is different compared with the strategy to maximise the geometric distance deviation for small values of $\Delta t < T_{NEO}$. From Fig. 3.2 it can be seen how the tangent component dominates early on for 2010 RF_{12}, later (for larger values of Δt) to be replaced by the normal component and finally by the tangent component again, aligning with the maximum δr behaviour.

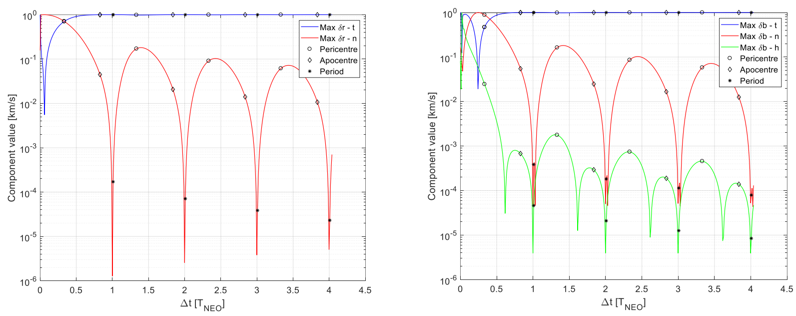

Fig. 3.2 Components of the maximum δr (left) and δb (right) deviation direction for 2010 RF_{12}

The oscillations of the normal and out-of-plane components in the neighbourhood of $\Delta t = kT_{NEO}$ stem from the sign change of those components (which translate to oscillations in the logarithmic representation).

3.3.2 Maximum ξ and ζ Deviation

In the case of the asteroid 2010 RF$_{12}$, the maximum $\delta\xi$ deviation direction alternates between out-of-plane and tangent throughout the period. Furthermore, the deviation proves very ineffective if performed along the tangent direction at $\Delta t = kT_{NEO}$, along the normal direction at $\Delta t = kT_{NEO} + T_{NEO}/2$ and along the out-of-plane direction for a value of Δt which varies for each NEO.

The direction of maximum ζ deviation follows similar rules as the δb maximisation (see Sect. 3.3.1). This result is consistent with the limited effect of the $\delta\xi$ maximisation beyond $\Delta t = T_{NEO}$, beyond which the optimal δb direction practically coincides with the $\delta\zeta$ one, as the ζ direction is related to the phasing, which is more easily modified than the ξ-related MOID [9].

These patterns can be observed in Fig. 3.3.

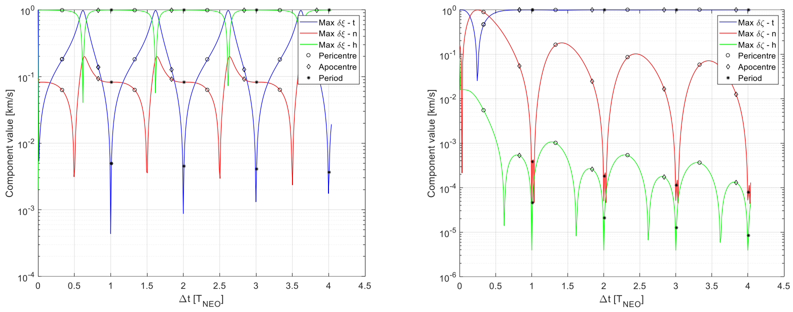

Fig. 3.3 Components of the maximum $\delta\xi$ (left) and $\delta\zeta$ (right) deviation direction for 2010 RF$_{12}$

3.4 Deflection Strategy to Avoid the Keyholes

An effective strategy to prevent a resonant return could be to deflect a NEO in such a way that its trajectory crosses the encounter b-plane far from any of the calculated keyholes. The distance from the keyholes is aimed at providing some robustness to the deflection action towards real-world effects, such as the real deflection not corresponding to the expected one. Assuming the asteroid could be deflected a sufficient amount of time before the first close approach, a deviation along the ζ-axis would be the most convenient, as is detailed in Sect. 3.3. For this reason, a target value of ζ can be selected based on the following criteria:

- Nominal encounter within a keyhole: the target ζ value is located halfway between the keyhole in question and the following one in the direction of increasing modulus of ζ (deflecting the NEO away from the Earth is a safer manoeuvre)
- Nominal encounter between two keyholes: the middle point between the two keyholes is selected as the target ζ value

The formulas presented in Sect. 3.2.2 can be used to determine the $\boldsymbol{\delta v}$ vector to be applied to the asteroid at the deflection coordinates in order to obtain the desired $\delta\zeta$ deviation on the b-plane through the following procedure:

1. Determination of the direction of maximum $\delta\zeta$ variation through the eigenvector method
2. Multiplying the modulus of the unitary $\boldsymbol{\delta v}$ vector by a factor $\delta\zeta / \delta\zeta_{eig}$, where $\delta\zeta_{eig}$ is the displacement along the ζ-axis obtained with the unitary $\boldsymbol{\delta v}$ vector (resulting from the eigenvector method)

It should be noted that the presented technique features some displacement along the ξ-axis (i.e. a change in the MOID) in addition to the desired one along the ζ-axis (i.e. a change in the encounter phasing), as the selected direction only guarantees the conditions to obtain the maximum value of $\delta\zeta$ for a given modulus of $\boldsymbol{\delta v}$ and value of Δt. The displacement along ξ can however be disregarded, as it is considerably smaller with respect to the one along ζ (see Sect. 3.3.2).

4 Results for the Avoidance of Resonant Encounters

A fundamental premise to the application in this chapter is that the results featured in this section are obtained through a R2BP propagation of the coordinates of both the asteroid and the Earth since their initial conditions, provided by NASA SPICE's ephemerides data [14], and are therefore not fully representative of the real conditions, all the while maintaining their general validity. This is done to better highlight the value of the theory derived in Sect. 3 as a preliminary theoretical design tool for a mission to subsequently be refined in the framework of the n-body problem.

4.1 Optimal Deflection

4.1.1 Optimal Deflection of 2010 RF_{12}

Let us consider a fictitious situation in which the 2095 encounter of 2010 RF_{12} with the Earth takes place in one of the b-plane's keyholes, specifically the (6,5) one, leading to a potentially dangerous return of the NEO in the year 2101. This condition would clearly be highly undesirable and a deflection mission to the asteroid would be recommended. The values of the Keplerian parameters assumed for both the Earth and the NEO are the ones previously detailed in Table 1.

An effective strategy to prevent the expected resonant return could be to deflect 2010 RF_{12} in such a way that its trajectory crosses the 2095 encounter b-plane far from any of the calculated keyholes. For the scope of this example, the asteroid is assumed to be deflected 400 days before the first close approach, allowing the application of the strategy described in Sect. 3.4. The target deflection will therefore be a $\delta\xi$ value equal to half the distance between the current keyhole (6,5) and the next one in the direction of increasing ζ (7,6).

Fig. 4.1 portrays the b-plane of the encounter; the resonant circles in the figure are computed analytically and therefore do not correspond with the numerical keyholes. The coordinates of the keyholes considered for the optimal deflection strategy, as well as the chosen target ζ value are shown as asterisk symbols. Finally, Fig. 4.2 displays the propagation of the post-fly-by conditions corresponding to the nominal conditions for the fictitious encounter and the deviated conditions obtained through the optimisation strategy in the form of the distance of the NEO from the Earth. The line corresponding to the nominal conditions clearly exhibits a return of the asteroid to the Earth, whereas the propagation of the deviated NEO suggests that the following encounter has been avoided.

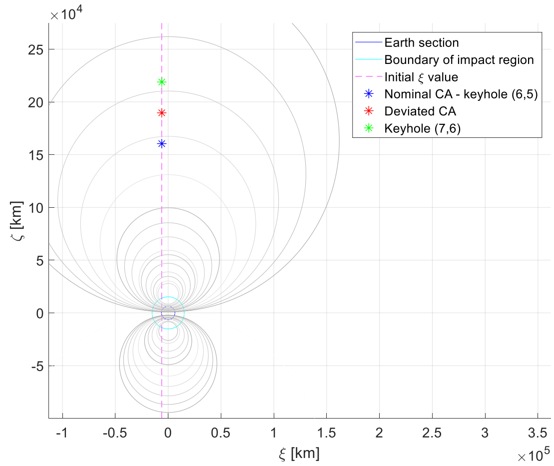

Fig. 4.1 B-plane of the 2095 close-approach of 2010 RF$_{12}$ with the Earth featuring the synthetic initial and deviated conditions

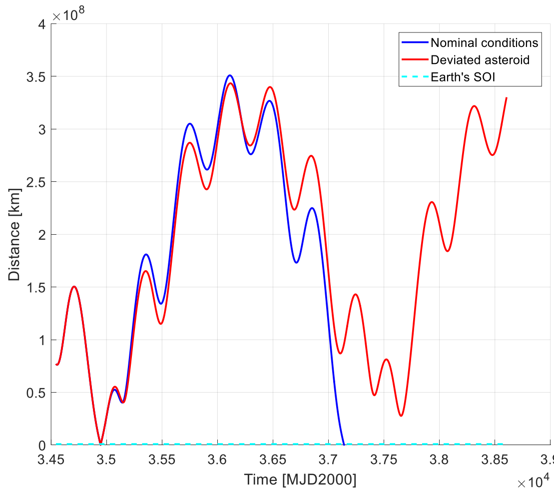

Fig. 4.2 Distance of the synthetic nominal and deviated 2010 RF$_{12}$ from the Earth

The optimal deviation, based on the procedure presented in this section and the assumed data, is obtained for $\boldsymbol{dv}_{tnh} = \{2.7284 \quad 0.0012 \quad -0.0002\} \cdot 10^{-1}\,\mathrm{m/s}$ (expressed in the tangent-normal-out-of-plane frame of the asteroid) even though a weaker deflection could be sufficient to avoid the following encounter. The computed value should be considered as having an *ideal* magnitude to provide a degree of robustness to the obtained result to face the disturbances due to effects that have not been considered, in particular the perturbation of the Keplerian heliocentric motion due to the presence of the other planets or the effects of the non-ideal deflection of the asteroid.

5 Conclusions

In this work, based on the theory behind the b-plane derived by Öpik [8] and Valsecchi et al. [4], a numerical technique to compute the b-plane keyholes is introduced and applied to the case of an elliptical Earth orbit and non-coincident position of a NEO with the planet's at the time of the encounter.

The deflection problem is modelled through the use of proximal motion equations and Gauss' planetary equations, providing a convenient analytical maximisation technique, following what had already been done in [7]. The maximisation technique was then extended to the impact parameter and the single axes of the b-plane and an analytical correlation between the deflection velocity vector and the displacement on the b-plane is presented. The correlation between the deflection and the resulting displacement along the ζ-axis of the b-plane was employed to define an optimal deflection strategy aimed at avoiding the keyholes, thus reducing the probability of a resonant return of the NEO to the Earth.

These tools have later been applied in the case of the optimal deflection of asteroid 2010 RF_{12}, aimed at avoiding the keyhole positions. It has been found that the deflection, if performed sufficiently in advance, is most effective if aligned with the direction tangent to the asteroid velocity and results in a displacement on the b-plane predominantly in the direction of the ζ-axis (corresponding to a variation in the close-encounter phasing).

It should be noted that a two-body approach has been considered to model the gravitational effects for the scope of this work, as stated throughout the present report. Such an approximation poses an obvious limitation to the validity of the obtained results, especially when considering a long-term propagation of the predicted effects. This approach was necessary in order to obtain some of the closed-form solutions presented in this paper, such as the aforementioned optimal deflection techniques and the exact return in the case of an encounter taking place in a keyhole. Nevertheless, the presented results retain their general validity, as discussed in the respective results sections, and can serve as a starting point from which to begin analysing a real close approach situation.

To tie to the previous limitation, future developments of this work could feature the development of a numerical approach to precisely determine the shape and position of keyholes in the case of an n-body propagation. A second possible addition to this work is represented by the propagation of a set of initial conditions instead of a single set of coordinates to account for the probability factor associated with the determination of an asteroid's orbital parameters. Furthermore, the definition of a more comprehensive strategy to determine the optimal deviation on the b-plane could be developed, possibly taking into consideration the timing of the expected returns associated with each keyhole, as well as the cost of each of the manoeuvres required to safely avoid them. Lastly, the modelling of the impact between the spacecraft and the NEO could be improved by considering the uncertainty due to the lack of precise knowledge about its shape, rotation and composition, giving rise to a breadth of possible resulting deviations.

Acknowledgements

The research leading to these results is part of the COMPASS project (Control of Orbit Manoeuvring through Perturbation for Application to Space Systems, grant agreement n° 679086) funded by the European Research Council (ERC) under the European Unions Horizon 2020 research and innovation programme. The authors acknowledge the use of the Milkyway High Performance Computing Facility, and associated support services at Politecnico di Milano, in the completion of this work.

Bibliography

[1] "NASA CNEOS - NEO Basics," [Online]. Available: https://cneos.jpl.nasa.gov/about/basics.html. [Accessed 6 July 2018].

[2] "NASA JPL - Discovery Statistics," [Online]. Available: https://cneos.jpl.nasa.gov/stats/totals.html. [Accessed 6 July 2018].

[3] C. R. Chapman and D. Morrison, "Impacts on the Earth by asteroids and comets: assessing the hazard," *Nature,* vol. 327, no. 6458, pp. 33-40, 1994.

[4] G. B. Valsecchi, A. Milani, G. F. Gronchi and S. R. Chesley, "Resonant returns to close approaches: Analytical theory," *Astronomy & Astrophysics,* pp. 1179-1196, 2003.

[5] "NEODyS-2 - 2010RF12 - Close Approaches," [Online]. Available: http://newton.dm.unipi.it/neodys/index.php?pc=1.1.8&n=2010RF12. [Accessed 8 July 2018].

[6] "ESA Cosmos - SMPAG - Statement on Asteroid Orbit Deflection Demonstrations," [Online]. Available: https://www.cosmos.esa.int/web/smpag/statement-on-asteroid-orbit-deflection-demonstration. [Accessed 8 July 2018].

[7] M. Vasile and C. Colombo, "Optimal Impact Strategies for Asteroid Deflection," *Journal of Guidance, Control, and Dynamics,* vol. 31, no. 4, 2008.

[8] E. J. Öpik, Interplanetary Encounters, New York: Elsevier, 1976.

[9] A. Bourdoux, "Characterization and hazard mitigation of resonant returning Near Earth Objects," ESA, 2005.

[10] G. B. Valsecchi, E. M. Alessi and A. Rossi, "An analytical solution for the swing-by problem," *Celestial Mechanics Dynamics and Astrodynamics,* no. 123, pp. 151-166, 2015.

[11] M. Petit, "Optimal Deflection of Resonant Near-Earth Objects Using the B-Plane, Master Thesis (Advisor: Prof. Camilla Colombo)," Politecnico di Milano, Milan, 2018.

[12] F. Letizia, C. Colombo, J. P. Van den Eynde and R. Jehn, "b-Plane Visualisation Tool for Uncertainty Evaluation," *AAS,* vol. 16, no. 438, 2016.

[13] F. Letizia, J. Van den Eynde and C. Colombo, "SNAPPshot ESA planetary protection compliance verification software, Final report," 2016.

[14] "NASA - JPL - NAIF - SPICE," [Online]. Available: https://naif.jpl.nasa.gov/naif/toolkit.html. [Accessed 9 July 2018].

[15] C. Colombo, "Optimal trajectory design for interception and deflection of Near Earth Objects, PhD Thesis," Glasgow Theses Service, 2010.

[16] D. K. Yeomans, S. Bhaskaran, S. B. Broschart, S. R. Chesley, P. W. Chodas, T. H. Sweetser and R. Schweickart, "Deflecting a Hazardous Near-Earth Object," in *1st IAA Planetary Defense Conference*, Granada, Spain, 2009.

[17] J. P. Sanchez, C. Colombo, M. Vasile and G. Radice, "Multicriteria comparison among several mitigation strategies for dangerous near-Earth objects," *Journal of Guidance, Control, and Dynamics,* vol. 32, no. 1, pp. 121-142, 2009.

[18] J. P. Sanchez and C. Colombo, "Impact Hazard Protection Efficiency by a Small Kinetic Impactor," vol. 50, no. 2, 2013.

[19] M. Romano, C. Colombo and J. M. Sánchez Pérez, "Efficient Planetary Protection Analysis for Interplanetary Missions," in *68th International Astronautical Congress*, Adelaide, Australia, 2018.

[20] D. Menzio and C. Colombo, "The Combined Lambert-Tisserand Method Applied to the Single Flyby Problem," in *68th International Astronautical Congress*, Adelaide, Australia, 2016.

[21] C. Colombo, M. Albano, R. Bertacin, M. M. Castronuovo, A. Gabrielli, E. Perozzi, G. Valsecchi and E. Vellutini, "Mission analysis for two potential asteroids threat scenarios: optimal impact strategies and thechnology evaluation," in *68th International Astronautical Congress*, Adelaide, Australia, 2017.

[22] A. Carusi, G. B. Valsecchi and R. Greenberg, "Planetary close encounters: Geometry of approach and post-encounter orbital parameters," *Celestial Mechanics and Dynamical Astronomy,* no. 49, pp. 111-131, 1990.